

Geophysical Research Letters

RESEARCH LETTER

10.1029/2021GL093184

Key Points:

- Madden-Julian Oscillation (MJO) statistical signals in general circulation model simulations depend on the size of large-scale precipitation tracking (LPT) systems
- Growth rate in the size of LPT systems at early stage determines the model simulated MJO statistical signals
- Comprehensive diagnostics of MJO simulations should include LPT systems as essential elements of the MJO

Supporting Information:

Supporting Information may be found in the online version of this article.

Correspondence to:

J. Ling,
lingjian@lasg.iap.ac.cn




Citation:

Chen, G., Chen, S. S., Ling, J., & Li, C. (2021). Large-scale precipitation systems: Essential elements of the Madden-Julian Oscillation. *Geophysical Research Letters*, 48, e2021GL093184. <https://doi.org/10.1029/2021GL093184>

Received 1 MAR 2021

Accepted 30 JUN 2021

Large-Scale Precipitation Systems: Essential Elements of the Madden-Julian Oscillation

Guiwan Chen^{1,2,3} , Shuyi S. Chen³, Jian Ling^{1,2} , and Chongyin Li¹ 

¹State Key Laboratory of Numerical Modelling for Atmospheric Sciences and Geophysical Fluid Dynamics, Institute of Atmospheric Physics, Beijing, China, ²University of Chinese Academy of Sciences, Chinese Academy of Sciences, Beijing, China, ³Department of Atmospheric Sciences, University of Washington, Seattle, WA, USA

Abstract Possible roles of large-scale precipitation on model simulations of the Madden-Julian Oscillation (MJO) were investigated using the Large-scale Precipitation Tracking (LPT) method. Individual LPT systems and eastward propagating MJO LPT systems were identified in both observations and 25 general circulation model (GCM) simulations. LPT systems show dominant eastward propagation over the Indian Ocean in the observation, whereas LPT systems are too stationary in GCM simulations. The MJO statistical signals in the model simulations are represented by the occurrence frequencies of LPT systems with a size of $\sim 4\text{--}9 \times 10^6 \text{ km}^2$ ($\sim 20\text{--}30^\circ$ in longitude and latitude) and a strength of $\sim 15\text{--}18 \text{ mm d}^{-1}$. Growth rate in size of LPT systems in early stage determines the size of LPT systems, which differentiates the MJO statistical signals among the GCM simulations. Comprehensive diagnostics of MJO simulations in GCMs should include both individual LPT systems as essential elements and the MJO statistical signals.

Plain Language Summary The Madden-Julian Oscillation (MJO) is the dominant mode of intraseasonal variabilities in the tropics and represents a major source of subseasonal predictability. A distinct feature of the MJO is its eastward propagating large-scale precipitating systems from the tropical Indian Ocean to the western-central Pacific. However, this feature is not well-reproduced by most general circulation models (GCMs). In this study, we explore possible reasons for why GCMs struggle to simulate the MJO eastward propagation by investigating the Large-scale Precipitation Tracking (LPT) systems. The results suggest that the problems of models in simulating the MJO are rooted in the LPT systems. The model capability of producing sufficient LPT systems that are large in size ($\sim 4\text{--}9 \times 10^6 \text{ km}^2$) and strong in strength ($\sim 15\text{--}18 \text{ mm d}^{-1}$) is essential for simulating the MJO. It is particularly important for models to capture the growth rate in size of LPT systems within the first several days after their initiation.

1. Introduction

Reproducing the observed Madden-Julian Oscillation (MJO, Madden & Julian, 1971, 1972) using general circulation models (GCMs) has been an unmet challenge (Ahn et al., 2020; Hung et al., 2013; Jiang et al., 2015). One distinct feature of the MJO is its eastward propagating large-scale precipitating systems from the tropical Indian Ocean to the western-central Pacific, which is not well represented in many GCM simulations. This weakness of models has been demonstrated through diagnoses using methods seeking statistical signals of the MJO, such as time-space spectra or their eastward versus westward power ratios, Empirical Orthogonal Function (EOF) analysis, and various types of regressions and composites (Kiladis et al., 2014; Liu et al., 2016; Waliser et al., 2009; Wheeler & Hendon, 2004; Wheeler & Kiladis, 1999; Zhang et al., 2006). Many previous studies have attempted to explain why most GCMs are incapable of reproducing this observed MJO feature. For this reason, new diagnostics metrics have been proposed to focus on physical processes (Benedict et al., 2014; Kim et al., 2014; Maloney, 2009) or dynamics (Wang et al., 2018) that are deemed critical to the MJO. These diagnostics have led to new physical insights on shortcomings in models that may lead to limited or no abilities of reproducing the MJO. These shortcomings are often attributed to systematic errors in the mean state (Gonzalez & Jiang, 2017; Inness et al., 2003; Kim et al., 2019; Sperber et al., 2005), precipitation, including its dependence on moisture (Kim et al., 2009).

Recently, a different MJO diagnostic concept has been introduced. Instead of relying primarily on statistical signals, individual MJO events can be identified by tracking their eastward propagation in precipitation

(Kerns & Chen, 2016, 2020; Ling et al., 2014; Zhang & Ling, 2017). One advantage of identifying individual MJO events is that many of their characteristics can be quantified. Propagation speeds, spatial scales, starting and ending longitudes and times all vary among different MJO events. These characteristics of individual MJO events are not available from MJO diagnostics based primarily on conventional statistics. Another advantage of identifying individual MJO events is that the procedure can also be used to identify other types of large-scale precipitation systems. The methods of identifying individual MJO events have led to a new perspective of MJO simulations by GCMs: Models that cannot produce statistical signals of the MJO can actually produce individual MJO events but infrequently (Chen et al., 2020; Ling et al., 2017, 2019). This new perspective raises a question: If a model cannot produce the MJO as frequently as observed, is the problem in simulating the MJO itself or in producing organized large-scale precipitation systems? In other words, does a model fail to produce the MJO as frequently as the observations because it cannot produce sufficient number of organized large-scale precipitation systems or because those systems cannot efficiently develop into the MJO even if they are produced by the models?

In this study, we aim to address these questions. We use the Large-scale Precipitation Tracking (LPT) method of Kerns and Chen (2020) to identify the large-scale precipitation systems in the observations and in GCM simulations (Section 2). The results are presented in Section 3. Conclusions and discussions are given in Section 4.

2. Data and Methods

Data of observed precipitation are from the 3-hourly TRMM Multisatellite Precipitation Analysis (TMPA) Version 7 product ($0.25^\circ \times 0.25^\circ$) from 1998 to 2018 (Huffman et al., 2007). Model outputs from 25 simulations of 20 years by 22 GCMs organized by the MJO Task Force (MJOTF) (Moncrieff et al., 2012; Waliser et al., 2012) and the GEWEX Atmospheric System Study (GASS) (Petch et al., 2011) project (MJOTF/GASS) were diagnosed. The simulation datasets are archived at 6-hour intervals with a horizontal resolution of 2.5° from 1991 to 2010. Detailed descriptions of these GCM simulations can be found in Jiang et al. (2015). For direct comparisons, the TMPA data were interpolated to the resolutions of the GCM simulations (2.5° and 6 hourly).

The LPT method developed by Kerns and Chen (2016) and improved by Kerns and Chen (2020) identifies the MJO in several steps. Precipitation in the tropics are mostly dominated by mesoscale convective systems (MCSs) (Houze, 2004). In order to identify a large-scale precipitation system that usually consists of a group of MCSs, Kerns and Chen (2020) first applied a 2-D Gaussian filtered (with a standard deviation of 5°) in both longitude and latitude using a 3-day running mean of the TMPA data. Individual Large-scale Precipitation Objects (LPOs) were identified as enclosed contours of 12 mm d^{-1} with a minimum size of four contiguous grid cells ($\sim 300,000 \text{ km}^2$) at a given time. The LPT system is defined as an LPO that can be tracked in time for at least 7 days. The LPT systems represent organized large-scale precipitation systems that exist longer than synoptic timescales. They may propagate in any direction or not propagate at all. The third step selects MJO LPT systems from the LPT systems that satisfy additional conditions. If an LPT system contains a predominantly eastward propagating segment with the convective centers being within the tropics (15°S – 15°N) for at least 7 days and propagate eastward for at least 10° in longitude, it is referred as an MJO LPT system. Details of this method can be found in Kerns and Chen (2020). Once individual LPT systems and MJO LPT systems are identified, their characteristics can be quantified. In this study, we mainly focus on three characteristics of the LPT systems: size, strength, and volumetric rainfall. The size of an LPT system is the mean of the areas of the enclosed contours of 12 mm d^{-1} from 3-day Gaussian filtered precipitation through its life span, while the strength and volumetric rainfall are the mean and integrated 3-day filtered rainfall inside the contours through its life span, respectively. For each GCM simulation, these three characteristics were averaged over all model simulated LPT systems.

We adopted a conventional measure of MJO statistical signals. It is the ratio of eastward versus westward intraseasonal (30–90 days) and planetary (zonal wavenumbers of 1–6) spectral power of precipitation anomalies in the tropics (15°S – 15°N). This ratio will be referred to as the E/W ratio. This measure has been commonly used in diagnosing MJO signals in observations (Zhang & Hendon, 1997) and GCM simulations (Hung et al., 2013; Zhang et al., 2006). A Kolmogorov-Smirnov (K-S) test was used to determine whether

the probability density functions (PDFs) between two sets of data are significantly different at the 95% confidence level, treating each LPT system or MJO LPT system as an independent data sample. The correlation results in this paper are obtained in the GCM simulations. A student-*t* test was used to determine if correlations between two variables are significantly at the 95% confidence level, counting each GCM simulation as an independent sample.

3. Results

We first compare characteristics of LPT systems in TRMM observations and GCM simulations. The global occurrence frequency of LPT systems is roughly 57 per year in TRMM observations. It is 60 per year in the simulations on average but varies among different simulations from 20 to 90 per year. There is no significant correlation between this global occurrence frequency of LPT systems and the E/W ratio in the simulations. As will be demonstrated later, this does not mean LPT systems are irrelevant to the MJO.

The individual and joint PDFs of zonal propagation speed, size, strength, and volumetric rainfall of the LPT systems from the TRMM observations and GCM simulations are shown in Figure 1. The observed LPT systems are mainly distributed over the tropical Indo-Pacific warm pool regions and South America (Kerns & Chen, 2020). There are three concentrated regions where most LPT systems in TRMM observations are first identified: the tropical Indian Ocean, western Pacific, and South America. The models are able to reproduce the LPT systems in the three regions. However, the PDFs of the starting longitudes of LPT systems in TRMM observations and the GCM simulations are significantly different (Figure 1a). Most models underproduce LPT systems over the Indian Ocean and overproduce them over the western Pacific.

In TRMM observations, most LPT systems initiated over the Indian Ocean propagate eastward while those initiated over the western Pacific propagate westward (color shading in Figure 1a). The westward propagation over the western Pacific is mainly contributed by LPT systems during boreal summer (not shown), which might be related to the quasi-biweekly oscillation initiated over the western Pacific and propagated westward (Kikuchi & Wang, 2009). The models cannot reproduce the distinct zonal propagation speed and direction between the Indian Ocean and western Pacific as shown in the observation. The model simulated LPT systems are generally more stationary in both ocean basins, and have much less (more) eastward propagating systems over the Indian Ocean (western Pacific) than the observations (Figure 1a).

The size of LPT systems produced by the models are significantly smaller than those in TRMM observations over the Indian Ocean (Figure 1b). The model simulated LPT systems are stronger than in TRMM observations (Figure 1c), while the volumetric rainfall of LPT systems are less in the simulations than in TRMM observations over both the Indian and Pacific basins (Figure 1d). These results provide a general comparison between the overall simulations and observations. The characteristics of the LPT systems in relation to the model's capability in producing the MJO in different models will be further examined.

The E/W ratios for each individual GCM simulations are shown in Figure 2. Most models produce weaker statistical signals of the MJO than TRMM observations. The E/W ratio is significantly correlated with the occurrence frequency of individual MJO LPT systems produced by the models (Figure 2a). This suggests that the occurrence frequency of individual MJO events can represent the signals of the MJO propagation in the simulations statistically as shown in previous studies (Chen et al., 2020; Ling et al., 2017, 2019). Most observed and model simulated MJO events are over the Indo-Pacific warm pool regions (Chen et al., 2020; Kerns & Chen, 2020; Ling et al., 2017; Zhang & Ling, 2017), therefore, the focus of the following analysis will be on LPT systems and MJO LPT systems initiated over the Indo-Pacific warm pool regions (40°E–180°, 15°S–15°N).

In the simulations, statistical signals of the MJO are correlated with the ratio of the occurrence frequency of MJO LPT systems to that of LPT systems (Figure 2b). More generally, the statistical signals of the MJO are closely related to how effective the models are in producing eastward propagating LPT systems (Figure 2c), as measured by the ratio of the occurrence frequency of eastward to westward propagating LPT systems. These results suggest that the capability of the models in producing eastward propagating LPT systems is important for model simulations of the MJO.

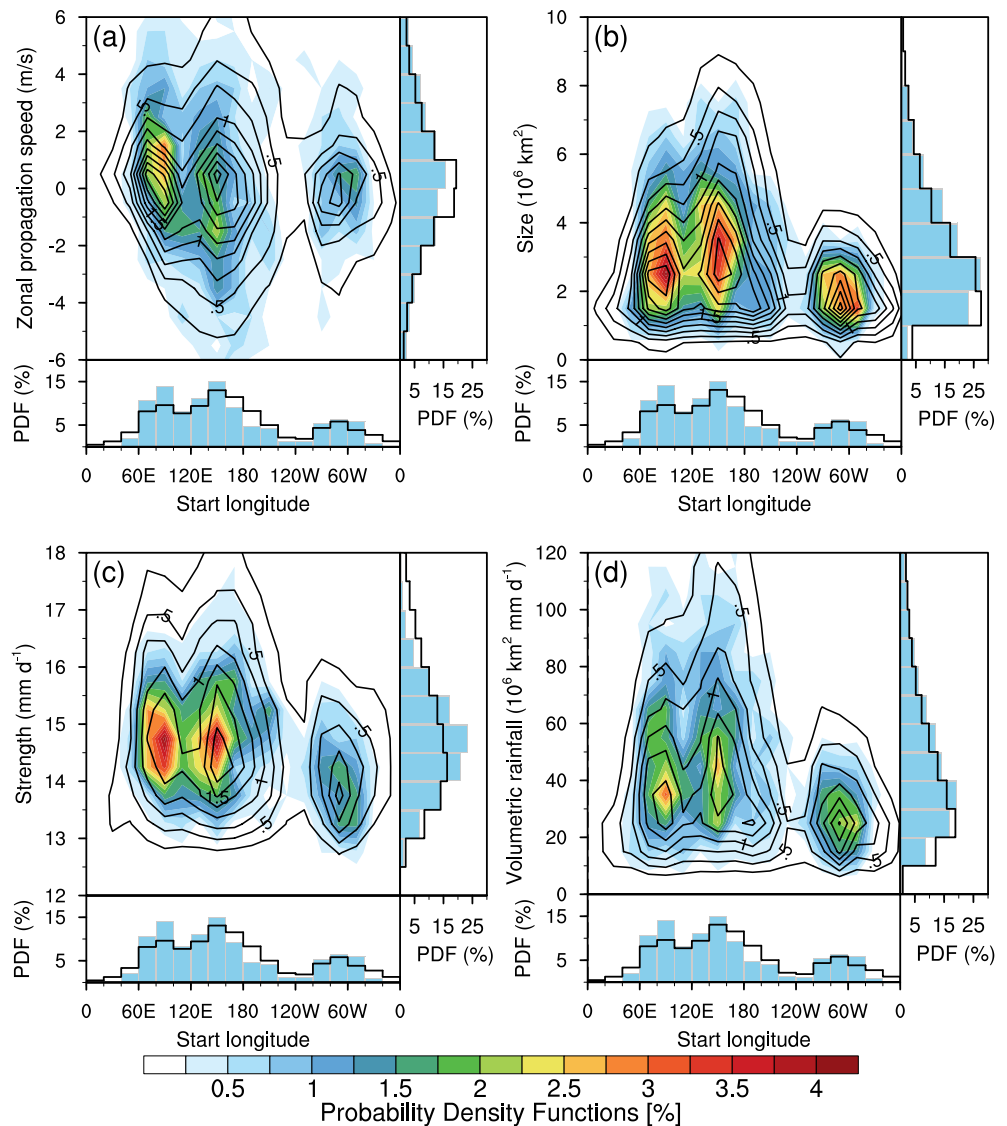


Figure 1. Individual and joint probability density functions (%) of (a) zonal propagation speed (m s^{-1}), (b) size (10^6 km^2), (c) strength (mm d^{-1}) and (d) volumetric rainfall ($10^6 \text{ km}^2 \text{ mm d}^{-1}$) of identified large-scale precipitation tracking systems in TRMM (blue bars and color shading) and the simulations (open bars and black contours; contours start from 0.25% with an interval of 0.25%) as the function of their starting longitude.

The sizes of LPT systems are also closely related to the statistical signals of the MJO in the simulations (Figure 2d), whereas there is no significant correlation between strength of LPT systems with MJO statistical signals (Figure 2e). The averaged volumetric rainfall of LPT systems is well correlated with the statistical signals of the MJO in the simulations (Figure 2f). These are clear signs that the models' capabilities of simulating the MJO are closely related to the LPT systems produced in the models. It is interesting to note that the TRMM observation lies under the best fit in Figure 2, and this may suggest that most GCMs need to overestimate the size, rain, and other properties of the LPT systems in order to reproduce similar observed MJO statistics.

The MJO statistical signals in the simulations are not related to their occurrence frequencies of LPT systems over all ocean basins, but they are closely related to other properties of LPT systems as shown in Figure 2. To explore whether the occurrence frequencies of the MJO LPT systems in the simulations are sensitive to their sizes and strengths, we compare the individual and joint distributions of occurrence frequencies of the MJO LPT systems as functions of their sizes and strengths in TRMM, top and bottom tier simulations

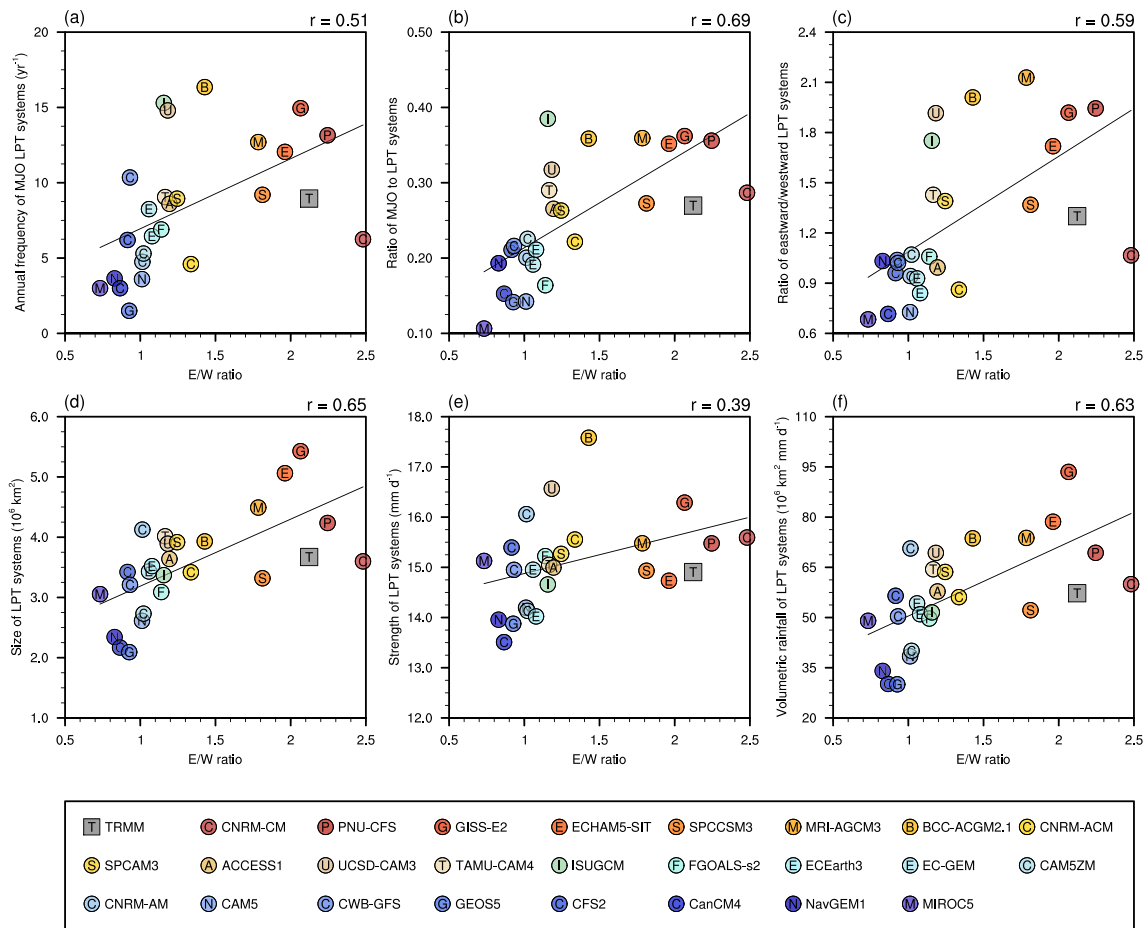


Figure 2. Scatter diagrams of the (a) occurrence frequency (yr^{-1}) of Madden-Julian Oscillation (MJO) large-scale precipitation tracking (LPT) systems, (b) ratio of the occurrence frequency of MJO LPT systems to that of LPT systems, (c) ratio of the occurrence frequency of the eastward to westward propagating LPT systems, (d) size (10^6 km^2), (e) strength (mm d^{-1}), and (f) volumetric rainfall ($10^6 \text{ mm d}^{-1} \text{ km}^2$) of LPT systems that start over the Indo-Pacific warm pool ($40^\circ\text{E}-180^\circ$; $15^\circ\text{S}-15^\circ\text{N}$) versus the E/W ratios in TRMM observations (gray triangle) and the simulations (color circles). The correlation coefficient is given at the upper-right corner (all significant at the 95% confidence level except for panel e). The straight line is a linear fit among all simulations.

(Figures 3a–3c). The top and bottom tier simulations are the top and bottom six simulations ranking by their E/W ratios as shown in Figure 2. In general, MJO LPT systems with greater size are also stronger (Figure 3a) in TRMM observations, both the top and bottom tier simulations can reproduce this feature. Compared with TRMM observations, the top tier simulations tend to produce MJO LPT systems more frequently and overestimate their size and strength (Figure 3b). The bottom tier simulations underestimate the occurrence frequency, size, and strength of MJO LPT systems (Figure 3c). The distribution of the correlation coefficients between occurrence frequencies of MJO LPT systems in the simulations and their E/W ratios as the function of size and strength is shown in Figure 3d. It is clear that the capabilities of the models to reproduce the MJO statistical signals are represented by the occurrence frequencies of MJO LPT systems with large size ($\sim 4-9 \times 10^6 \text{ km}^2$) and strong strength ($\sim 15-18 \text{ mm d}^{-1}$).

The distributions of occurrence frequencies for LPT systems (Figures 3e–3g) show similar patterns as the MJO LPT systems. But the LPT systems are generally smaller in size and weaker in strength compared with the MJO LPT systems. In general, the models with higher MJO simulation skill tend to produce more LPT systems with large size ($\sim 4-9 \times 10^6 \text{ km}^2$) and strong strength ($\sim 15-18 \text{ mm d}^{-1}$), while those with lower simulation skill tend to produce more LPT systems with small size ($\sim 1-2 \times 10^6 \text{ km}^2$) and weak strength ($\sim 12-14 \text{ mm d}^{-1}$) (Figure 3h). This dipole correlation distribution in Figure 3h explains why there is no significant correlation between strength of LPT systems and E/W ratios in the simulations (Figure 2e). The results suggest that large and strong LPT systems are more likely to develop into MJO LPT systems. Models

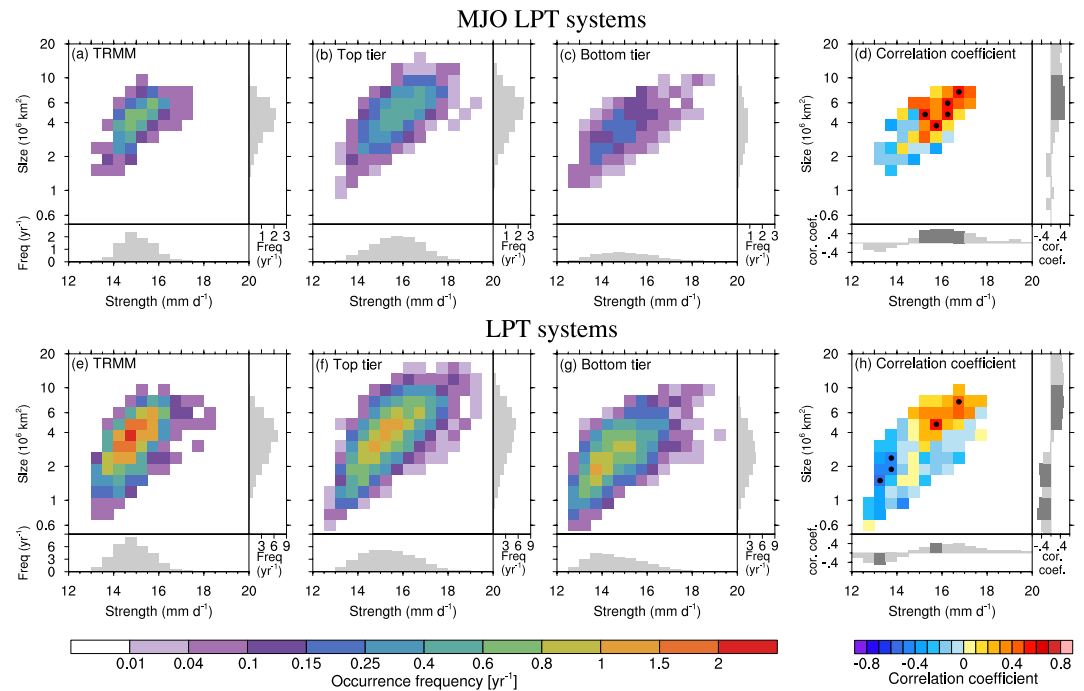


Figure 3. Individual and joint distributions of the occurrence frequencies (yr^{-1}) of (a–c) the Madden-Julian Oscillation large-scale precipitation tracking (LPT) systems, and (e–h) the LPT systems in (a, e) TRMM, (b, f) top, and (c, g) bottom tier simulations, and (d, g) the correlation coefficients between their occurrence frequencies and the E/W ratios as functions of size and strength in the simulations. Dots and dark gray bars mark the results that are significant at the 95% confidence level.

that can produce sufficient number of large and strong LPT systems tend to produce stronger statistical signals of the MJO propagation. It is worth noting that the top tier simulations tend to overestimate the size and strength of the LPT systems (Figure 3f). For the simulations excluding the top and bottom simulations, it is true that their averages of characteristics for LPT systems are closer to TRMM observations as shown in Figure 2. But they tend to underestimate the occurrence frequency of LPT systems with large size and strong strength, and the distributions of the characteristics for the LPT systems they produced are also quite different from TRMM observations (not shown).

To explain the differences in sizes of MJO LPT systems as well as LPT systems among the simulations, we further compare the evolutions of the sizes of MJO LPT systems and LPT systems in TRMM observations and the simulations (Figure 4). The sizes of MJO LPT systems in TRMM increase rapidly in their sizes after initiation, they grow from $1\text{--}2 \times 10^6 \text{ km}^2$ at initiation into $4\text{--}5 \times 10^6 \text{ km}^2$ in 7 days. After that, their sizes start to decay. Both the sizes of MJO LPT systems in the top and bottom tier simulation show similar evolution pattern, but with different magnitude. The sizes of MJO LPT systems in the top tier simulations are greater than that in the bottom tier simulations after initiation. The sizes of MJO LPT systems in the top tier simulations increase more rapidly within 7 days after their initiation and decay more quickly afterwards compared with those in the bottom tier simulations (Figure 4b).

In general, the LPT systems in the top tier simulations tend to grow quickly in size within 5 days after their initiation and decay quickly afterwards (Figures 4c and 4d), whereas the bottom tier simulations cannot organize the precipitation systems into large-scale effectively. The faster the growth rate of LPT systems' sizes at the early stage, the larger the sizes of LPT systems may become, which can then increase their chance to develop into MJO LPT systems. Same comparisons for non-MJO LPT systems (not shown) have similar results and the overall sizes of LPT systems are smaller. If an LPT system cannot grow in size quickly, it is unlikely to develop into an MJO LPT system. Similarly, if a model cannot organize its precipitation systems into large-scale effectively, it is unlikely to be able to reproduce the MJO statistics.

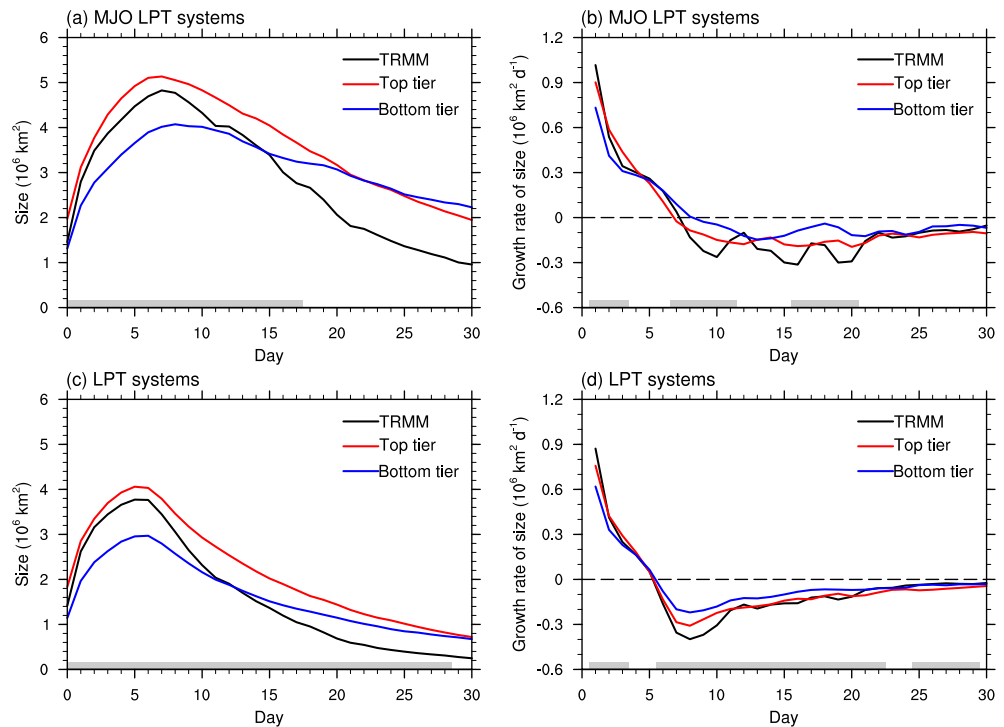


Figure 4. Time evolutions of (a, c) size (10^6 km^2) and (b, d) grow rate of size ($10^6 \text{ km}^2 \text{ d}^{-1}$) for (top panel) Madden-Julian Oscillation (MJO) large-scale precipitation tracking (LPT) systems and (bottom) LPT systems in TRMM, top tier simulations and bottom tier simulations. Day 0 is the day when MJO LPT systems and LPT systems are initiated; gray bars mark the days when differences between the top tier and bottom tier simulations are significant at the 95% confidence level.

4. Summary and Discussions

This study investigates the role of organized large-scale precipitation on the GCM simulations of the MJO using the Large-scale Precipitation Tracking (LPT) method of Kerns and Chen (2020). Individual LPT systems are identified as an area of contiguous precipitation $>12 \text{ mm d}^{-1}$ at least $300,000 \text{ km}^2$ that are trackable for at least 7 days. The LPT systems can propagate in any direction. Some of them move predominately eastward and become MJO LPT systems. The results show that the LPT systems are essential elements of the MJO, which may be considered as necessary conditions for the MJO. This new diagnostic method is used to evaluate the MJO simulation in the GCM simulations. Our results show that the top tier models that can reproduce stronger MJO propagation signals in statistics are generally capable of producing better LPT systems with size, growth rate, strength, and volumetric rainfall than those in the bottom tier models. The results indicate that shortcomings of GCM simulations in reproducing the MJO statistics are rooted in their deficient productions of LPT systems.

The MJO statistical signals in the models are not related to the global occurrence frequency of LPT systems. But they are closely related to the occurrence frequency of LPT systems with size around $4\text{--}9 \times 10^6 \text{ km}^2$ and strength around $15\text{--}18 \text{ mm d}^{-1}$. Further analysis indicates that if the models produce LPT systems that grow quickly in size at early stage, they tend to produce sufficient numbers of LPT systems with larger size that are more likely to develop into MJO LPT systems. As the result, models that can grow the size of their LPT systems more quickly tend to produce stronger MJO propagation in statistics. Future studies should investigate the controlling mechanism for the growth rate in size of LPT systems.

The criteria of selecting MJO LPT systems from LPT systems cannot be determined objectively. There is a peak in the joint PDF for zonal propagation speed and size centered at $0\text{--}1 \text{ ms}^{-1}$ and $2\text{--}3 \times 10^6 \text{ km}^2$ ($\sim 12\text{--}16^\circ$ in longitude and latitude) for LPT systems in TRMM observations (Figure S1a). Distributions of the zonal speed and size of LPT systems from the peak are continuous without any hint that would suggest

a threshold that can be selected objectively to pick MJO LPT systems from the LPT systems. This appears to be at odd with the MJO signals in the time-space spectrum as a spectral peak that is distinctively separated from those of lower and higher frequencies (Zhang, 2005). But this spectral peak would completely disappear if time (or frequency) is converted into zonal speed. This smooth distribution in the zonal speed of identified large-scale precipitation events, previously found by Zhang and Ling (2017), is consistent to the notion of the continuum nature of the MJO and other tropical low-frequency perturbations, such as the equatorial Kelvin wave (Roundy, 2012).

The continuum nature and difficulty of objectively selecting MJO is not unique to the LPT method. Zhang and Ling (2017) used a different tracking method to identify individual MJO events using an arbitrary threshold in the zonal propagation speed (3 m s^{-1}). This lack of objective selection of MJO also exists when one tries to use the most common MJO metric, the Real-time Multivariable MJO (RMM) index (Wheeler & Hendon, 2004). In the literature, with very few exceptions, MJO events are identified when the amplitude of the RMM index is greater than one. The peak in the PDF of the RMM amplitude near one (bars at the abscissa of Figure S1b) does not make its choice as a threshold objective because the distribution goes smoothly in both directions from there. Adding extra information, such as consecutive days with the RMM amplitude remains greater than a given initial value, does not help (Figure S1b). Unfortunately, the arbitrary choice of selecting MJO using RMM amplitude greater than one has become a common practice in studies of the MJO with the only justification that it had been used previously by others.

Kerns and Chen (2020) indicated that the MJO contributes to up to 40%–50% of the precipitation climatology over the Indo-Pacific warm pool regions. For fair comparisons among the models, we applied the LPT method based on the total precipitation in this study. One might concern that using the same threshold of 12 mm d^{-1} is inappropriate, as the precipitation patterns among the models differ from the observation. The MJO is usually treated as a variability (Madden & Julian, 1971, 1972), therefore, most previous studies were conducted based on filtered or non-filtered anomalous data. To avoid the above-mentioned concerns, we have conducted similar analysis but based on anomalous precipitation. The annual cycle of precipitation in each simulation and TRMM observations was first removed. The averaged one standard deviation of the 3-day Gaussian filtered precipitation anomalies over the warm pool regions was used as the threshold to identify Large-scale Precipitation Objects, LPT systems and MJO LPT systems. We reproduce the results in Figure 3 but using the normalized strength (normalized by the threshold used for tracking the LPT systems), the results also suggest that the MJO statistical signals in GCM simulations are closely related to the size and normalized strength of LPT systems they reproduced (Figure S2).

Data Availability Statement

The TMPA data are provided by the NASA/Goddard Space Flight Center and archived at the NASA GES DISC online (https://disc.gsfc.nasa.gov/datasets/TRMM_3B42_7/summary). The MJOTF/GASS twenty-year climate simulations are provided by the MJOTF/GASS MJO global model comparison project (<https://www.cgd.ucar.edu/projects/yotc/mjo/vertical.html>). The RMM index values were obtained from the Australian Bureau of Meteorology and are available via their website (<http://www.bom.gov.au/climate/mjo/>).

References

- Ahn, M. S., Kim, D., Kang, D., Lee, J., Sperber, K. R., Gleckler, P. J., et al. (2020). MJO propagation across the Maritime Continent: Are CMIP6 models better than CMIP5 models? *Geophysical Research Letters*, *47*(11), e2020GL087250. <https://doi.org/10.1029/2020gl087250>
- Benedict, J. J., Maloney, E. D., Sobel, A. H., & Frierson, D. M. (2014). Gross moist stability and MJO simulation skill in three full-physics GCMs. *Journal of the Atmospheric Sciences*, *71*(9), 3327–3349. <https://doi.org/10.1175/jas-d-13-0240.1>
- Chen, G., Ling, J., Li, C., Zhang, Y., & Zhang, C. (2020). Barrier effect of the Indo-Pacific Maritime Continent on MJO propagation in observations and CMIP5 models. *Journal of Climate*, *33*, 5173–5193. <https://doi.org/10.1175/jcli-d-19-0771.1>
- Gonzalez, A. O., & Jiang, X. (2017). Winter mean lower tropospheric moisture over the Maritime Continent as a climate model diagnostic metric for the propagation of the Madden-Julian oscillation. *Geophysical Research Letters*, *44*(5), 2588–2596. <https://doi.org/10.1002/2016gl072430>
- Houze, R. A. (2004). Mesoscale convective systems. *Reviews of Geophysics*, *42*, RG4003. <https://doi.org/10.1029/2004rg000150>
- Huffman, G. J., Bolvin, D. T., Nelkin, E. J., Wolff, D. B., Adler, R. F., Gu, G., et al. (2007). The TRMM multisatellite precipitation analysis (TMPA): Quasi-global, multiyear, combined-sensor precipitation estimates at fine scales. *Journal of Hydrometeorology*, *8*(1), 38–55. <https://doi.org/10.1175/jhm560.1>
- Hung, M. P., Lin, J. L., Wang, W., Kim, D., Shinoda, T., & Weaver, S. J. (2013). MJO and convectively coupled equatorial waves simulated by CMIP5 climate models. *Journal of Climate*, *26*(17), 6185–6214. <https://doi.org/10.1175/jcli-d-12-00541.1>

Acknowledgments

The authors thank two anonymous reviewers for their constructive comments that helped improve the manuscript. We are grateful to Chidong Zhang of NOAA/PMEL for his input during the course of the study and suggestions on the content of the manuscript. We also thank Brandon Kerns of UW for providing assistance in the LPT analysis. This study was supported by the National Key R&D Program of China through Grants 2018YFC1505901 and 2018YFA0606203, the National Nature Science Foundation of China through Grant No. 41922035, 41575062, 41520104008, Key Research Program of Frontier Sciences of CAS through Grant No. QYZDB-SSW-DQC017, the External Cooperation Program of BIC, Chinese Academy of Sciences through Grant No. 134111KYSB20200020, and the NOAA CVP Research grant NA15OAR4320063.

- Inness, P. M., Slingo, J. M., Guilyardi, E., & Cole, J. (2003). Simulation of the Madden-Julian oscillation in a coupled general circulation model. Part II: The role of the basic state. *Journal of Climate*, *16*(3), 365–382. [https://doi.org/10.1175/1520-0442\(2003\)016<0365:sotmjo>2.0.co;2](https://doi.org/10.1175/1520-0442(2003)016<0365:sotmjo>2.0.co;2)
- Jiang, X., Waliser, D. E., Xavier, P. K., Petch, J., Klingaman, N. P., Woolnough, S. J., et al. (2015). Vertical structure and physical processes of the Madden-Julian oscillation: Exploring key model physics in climate simulations. *Journal of Geophysical Research: Atmospheres*, *120*(10), 4718–4748. <https://doi.org/10.1002/2014jd022375>
- Kerns, B. W., & Chen, S. S. (2016). Large-scale precipitation tracking and the MJO over the Maritime Continent and Indo-Pacific warm pool. *Journal of Geophysical Research: Atmospheres*, *121*(15), 8755–8776. <https://doi.org/10.1002/2015jd024661>
- Kerns, B. W., & Chen, S. S. (2020). A 20-year climatology of Madden-Julian oscillation convection: Large-scale precipitation tracking from TRMM-GPM rainfall. *Journal of Geophysical Research*, *126*(7). <https://doi.org/10.1029/2019jd032142>
- Kikuchi, K., & Wang, B. (2009). Global perspective of the quasi-biweekly oscillation. *Journal of Climate*, *22*(6), 1340–1359. <https://doi.org/10.1175/2008jcli2368.1>
- Kiladis, G. N., Dias, J., Straub, K. H., Wheeler, M. C., Tulich, S. N., Kikuchi, K., et al. (2014). A comparison of OLR and circulation-based indices for tracking the MJO. *Monthly Weather Review*, *142*(5), 1697–1715. <https://doi.org/10.1175/mwr-d-13-00301.1>
- Kim, D., Kug, J. S., & Sobel, A. H. (2014). Propagating versus nonpropagating Madden-Julian oscillation events. *Journal of Climate*, *27*(1), 111–125. <https://doi.org/10.1175/jcli-d-13-00084.1>
- Kim, D., Sperber, K., Stern, W., Waliser, D., Kang, I. S., Maloney, E., et al. (2009). Application of MJO simulation diagnostics to climate models. *Journal of Climate*, *22*(23), 6413–6436. <https://doi.org/10.1175/2009jcli3063.1>
- Kim, H., Janiga, M. A., & Pegion, K. (2019). MJO Propagation processes and mean biases in the SubX and S2S reforecasts. *Journal of Geophysical Research: Atmospheres*, *124*, 9314–9331. <https://doi.org/10.1029/2019jd031139>
- Ling, J., Bauer, P., Bechtold, P., Beljaars, A., Forbes, R., Vitart, F., et al. (2014). Global versus local MJO forecast skill of the ECMWF model during DYNAMO. *Monthly Weather Review*, *142*(6), 2228–2247. <https://doi.org/10.1175/mwr-d-13-00292.1>
- Ling, J., Zhang, C., Wang, S., & Li, C. (2017). A new interpretation of the ability of global models to simulate the MJO. *Geophysical Research Letters*, *44*(11), 5798–5806. <https://doi.org/10.1002/2017gl073891>
- Ling, J., Zhao, Y., & Chen, G. (2019). Barrier effect on MJO propagation by the Maritime Continent in the MJOTF/GASS models. *Journal of Climate*, *32*, 5529–5547.
- Liu, P., Zhang, Q., Zhang, C., Zhu, Y., Khairoutdinov, M., Kim, H. M., et al. (2016). A revised real-time multivariate MJO index. *Monthly Weather Review*, *144*(2), 627–642. <https://doi.org/10.1175/mwr-d-15-0237.1>
- Madden, R. A., & Julian, P. R. (1971). Detection of a 40–50 day oscillation in the zonal wind in the tropical Pacific. *Journal of the Atmospheric Sciences*, *28*(5), 702–708. [https://doi.org/10.1175/1520-0469\(1971\)028<0702:doadoi>2.0.co;2](https://doi.org/10.1175/1520-0469(1971)028<0702:doadoi>2.0.co;2)
- Madden, R. A., & Julian, P. R. (1972). Description of global-scale circulation cells in the tropics with a 40–50 day period. *Journal of the Atmospheric Sciences*, *29*(6), 1109–1123. [https://doi.org/10.1175/1520-0469\(1972\)029<1109:dogscc>2.0.co;2](https://doi.org/10.1175/1520-0469(1972)029<1109:dogscc>2.0.co;2)
- Maloney, E. D. (2009). The moist static energy budget of a composite tropical intraseasonal oscillation in a climate model. *Journal of Climate*, *22*(3), 711–729. <https://doi.org/10.1175/2008jcli2542.1>
- Moncrieff, M. W., Waliser, D. E., Miller, M. J., Shapiro, M. A., Asrar, G. R., & Caughey, J. (2012). Multiscale convective organization and the YOTC virtual global field campaign. *Bulletin of the American Meteorological Society*, *93*(8), 1171–1187. <https://doi.org/10.1175/bams-d-11-00233.1>
- Petch, J., Waliser, D., Jiang, X., Xavier, P. K., & Woolnough, S. (2011). A global model intercomparison of the physical processes associated with the Madden-Julian oscillation. *GEWEX News*, *21*(3), 3–5.
- Roundy, P. E. (2012). Observed structure of convectively coupled waves as a function of equivalent depth: Kelvin waves and the Madden-Julian oscillation. *Journal of the Atmospheric Sciences*, *69*(7), 2097–2106. <https://doi.org/10.1175/jas-d-12-03.1>
- Sperber, K. R., Gualdi, S., Legutke, S., & Gayler, V. (2005). The Madden-Julian oscillation in ECHAM4 coupled and uncoupled general circulation models. *Climate Dynamics*, *25*(2–3), 117–140. <https://doi.org/10.1007/s00382-005-0026-3>
- Waliser, D. E., Moncrieff, M. W., Burridge, D., Fink, A. H., Gochis, D., Goswami, B. N., et al. (2012). The “year” of tropical convection (May 2008–April 2010): Climate variability and weather highlights. *Bulletin of the American Meteorological Society*, *93*(8), 1189–1218. <https://doi.org/10.1175/2011bams3095.1>
- Waliser, D. E., Sperber, K., Hendon, H., Kim, D., Maloney, E., Wheeler, M., et al. (2009). MJO simulation diagnostics. *Journal of Climate*, *22*(11), 3006–3030. <https://doi.org/10.1175/2008jcli2731.1>
- Wang, B., Lee, S. S., Waliser, D. E., Zhang, C., Sobel, A., Maloney, E., et al. (2018). Dynamics-oriented diagnostics for the Madden-Julian Oscillation. *Journal of Climate*, *31*(8), 3117–3135.
- Wheeler, M. C., & Hendon, H. H. (2004). An all-season real-time multivariate MJO index: Development of an index for monitoring and prediction. *Monthly Weather Review*, *132*(8), 1917–1932. [https://doi.org/10.1175/1520-0493\(2004\)132<1917:aarmmi>2.0.co;2](https://doi.org/10.1175/1520-0493(2004)132<1917:aarmmi>2.0.co;2)
- Wheeler, M. C., & Kiladis, G. N. (1999). Convectively coupled equatorial waves: Analysis of clouds and temperature in the wavenumber–frequency domain. *Journal of the Atmospheric Sciences*, *56*(3), 374–399. [https://doi.org/10.1175/1520-0469\(1999\)056<0374:ccewao>2.0.co;2](https://doi.org/10.1175/1520-0469(1999)056<0374:ccewao>2.0.co;2)
- Zhang, C. (2005). Madden-Julian oscillation. *Reviews of Geophysics*, *43*(2). <https://doi.org/10.1029/2004rg000158>
- Zhang, C., Dong, M., Gualdi, S., Hendon, H. H., Maloney, E. D., Marshall, A., et al. (2006). Simulations of the Madden-Julian oscillation in four pairs of coupled and uncoupled global models. *Climate Dynamics*, *27*(6), 573–592. <https://doi.org/10.1007/s00382-006-0148-2>
- Zhang, C., & Hendon, H. H. (1997). Propagating and standing components of the intraseasonal oscillation in tropical convection. *Journal of the Atmospheric Sciences*, *54*(6), 741–752. [https://doi.org/10.1175/1520-0469\(1997\)054<0741:pascot>2.0.co;2](https://doi.org/10.1175/1520-0469(1997)054<0741:pascot>2.0.co;2)
- Zhang, C., & Ling, J. (2017). Barrier effect of the Indo-Pacific Maritime Continent on the MJO: Perspectives from tracking MJO precipitation. *Journal of Climate*, *30*(9), 3439–3459. <https://doi.org/10.1175/jcli-d-16-0614.1>